# Measurement of the coefficient of permeability for a deformable unsaturated soil using a triaxial permeameter

**Shangyan Huang, D.G. Fredlund, and S.L. Barbour**

**Abstract**: The development of a specially designed triaxial permeameter for the measurement of the coefficient of permeability of deformable unsaturated soils is presented in this paper. The triaxial permeameter makes it possible to directly measure the coefficient of permeability at various combinations of net normal stresses and matric suction values. The volume change of the soil specimen during the permeability measurement can also be monitored. The performance of the permeameter is demonstrated for a group of tests conducted on slurried specimens of a silty sand.

*Key words*: unsaturated soil, coefficient of permeability, triaxial permeameter, volume change.

**Résumé** : Le développement d'un perméamètre triaxial spécialement conçu pour la mesure du coefficient de perméabilité des sols non saturés déformables est l'objet de cet article. Le perméamètre triaxial rend possible la mesure directe du coefficient de perméabilité pour diverses combinaisons de contraintes normales nettes et pour différentes valeurs de la succion matricielle. Le changement de volume de l'échantillon de sol pendant la mesure de perméabilité peut également être suivi. Le bon fonctionnement du perméamètre est démontré par un ensemble d'essais effectués sur des spécimens de sable silteux à l'état de boues.

*Mots clés* : sols non saturés, coefficient de perméabilité, perméamètre triaxial, changement de volume.

[Traduit par la Rédaction]

## Introduction

The coefficient of permeability of a *saturated* soil can be described as a function of void ratio. The coefficient of permeability for an *unsaturated* soil with a relatively incompressible structure can be described as a function of the degree of saturation (Fredlund and Rahardjo 1993). However, from an engineering standpoint, soils are deformable, and the coefficient of permeability function for a deformable unsaturated soil should incorporate the influence of changes in both the void ratio and the degree of saturation. The degree of saturation of a specimen is difficult to control, predict, or measure. The relationship between the degree of saturation (or volumetric water content) and matric suction is represented by the soil–water characteristic curve for the soil (Fredlund and Rahardjo 1993). Consequently, the coefficient of permeability of an unsaturated soil can also be defined as a function of a known stress state (i.e., matric suction).

A number of methods have been proposed for measuring the coefficient of permeability of an unsaturated soil (Klute 1965, 1972; Klute and Dirksen 1986). The steady-state method has proven to be the most straightforward. Two types of steady-state techniques have been proposed. One technique controls the hydraulic head while the other technique controls the discharge through the specimen (Klute and Dirksen 1986). The controlled head, steady-state technique appears to be most commonly used. A number of variations of this method have been developed (e.g., Corey 1957; Klute 1965, 1972; Klute and Dirksen 1986). Some of these methods were developed to measure the coefficient of permeability with respect to water and air phases simultaneously. Other methods have been developed to measure only the coefficient of permeability with respect to the water phase.

Barden and Pavlakis (1971) developed a triaxial permeameter to simultaneously measure the coefficient of permeability with respect to water and air phases. A triaxial cell was used to simulate the in situ stress conditions. The total stress, pore-water pressure, and pore-air pressure were controlled independently. No attempt was made to measure total volume change of the soil specimen.

Huang et al. (1998) proposed a theoretical model for the coefficient of permeability function for a deformable unsaturated soil. A permeameter was developed that can measure the coefficient of permeability of an unsaturated deformable soil to verify the proposed model. The design of the triaxial permeameter cell is described in this paper. A number of permeability tests conducted using this permeameter are presented and are used to evaluate the performance of the triaxial permeameter.

Received October 31, 1997. Accepted January 23, 1998.

**S. Huang, D.G. Fredlund, and S.L. Barbour**. Department of Civil Engineering, 57 Campus Drive, University of Saskatchewan, Saskatoon, SK S7N 5A9, Canada.

## Equipment

The developed triaxial permeameter system consists of a triaxial cell and a control board with copper plumbing connections. The triaxial cell was a modification of the

**Fig. 1.** General assembly of the triaxial permeameter cell (modified from Ho 1988).

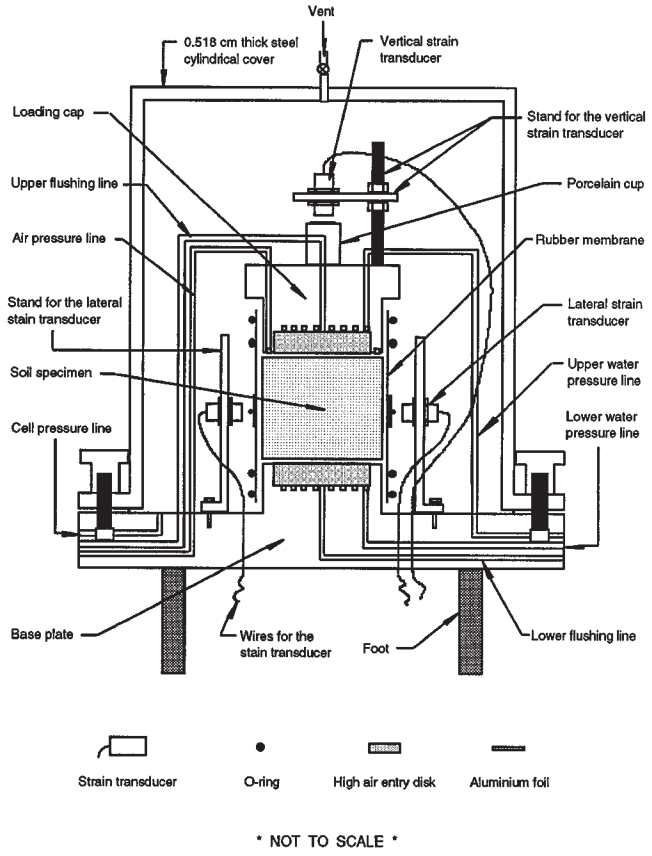


**Fig. 2.** Schematic layout for the flexible-wall permeability tests.

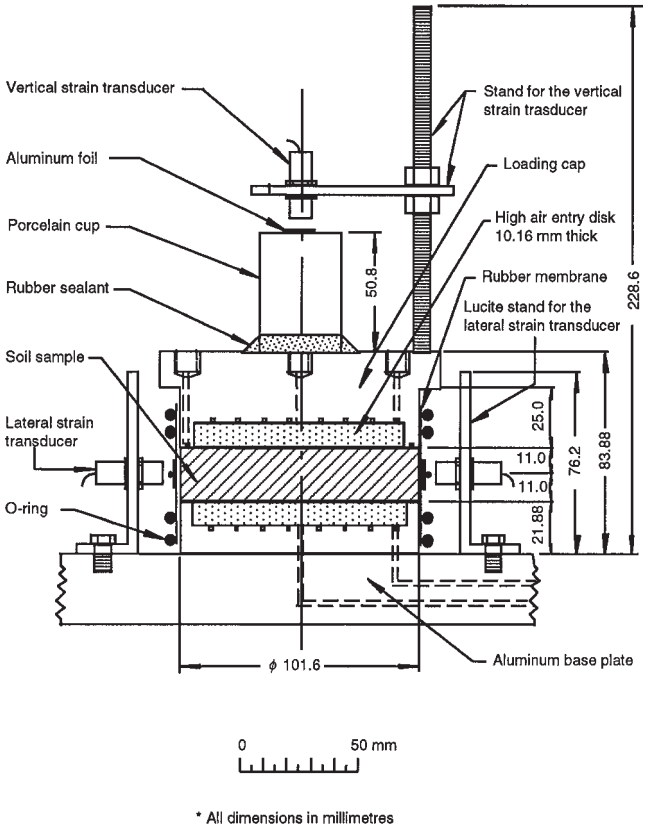


stress-controlled isotropic cell developed by Ho (1988). The original cell was used to investigate the deformation of unsaturated soils associated with changes in matric suction. The basic requirements for the system and the details of the system are described below.

## Requirements for the triaxial permeameter system

To measure the coefficient of permeability of a deformable unsaturated soil at different stress states, the triaxial permeameter system was developed to meet the following requirements. The system should be capable of

(*i*) independently controlling (and measuring) the total stress, the pore-air pressure and the pore-water pressure

(*ii*) controlling (and monitoring) the differential pressure or hydraulic head applied to the water phase

(*iii*) measuring accurately the inflow and outflow water volumes

(*iv*) flushing the diffused air bubbles which accumulate outside of the high air-entry disks and periodically measuring the volume of the diffused air; and

(*v*) monitoring the change in volume of the soil specimen during permeability tests.

The triaxial permeameter system was developed to meet these requirements.

## Description of the triaxial permeameter cell

The layout of the triaxial permeameter cell is shown in Fig. 1. The cell consists of a steel cylindrical cover, an aluminum base plate, and aluminum loading cap. The steel cylindrical cover is the same as that used in the original design and can sustain a pressure up to 1 500 kPa (Ho 1988).

The base plate designed by Ho (1988) was modified. A 10.1-mm thick, 90.0-mm diameter, 1-bar high-flow high air-entry disk was installed. A new aluminum loading cap was designed to include a 10.1-mm thick, 88.0-mm diameter, 1-bar high-flow high air-entry disk (Fig. 1). The 1-bar high flow, high air-entry disk has a coefficient of permeability ranging from $2.0 \times 10^{-8}$ to $2.5 \times 10^{-8}$ m/s. A commercial glue, "Epoxy 907"[1] was used to seal the high air-entry disks onto the base plate and the cap. A groove, 2.0-mm wide and 2.0-mm deep, was made on the cap for applying the pore-air pressure to the specimen. A similar spiral groove was made on both the pedestal and the cap for flushing air bubbles that accumulate outside the high air-entry disks as a result of diffusion. Air bubbles that accumulate in the pore-water pressure lines produce an error in the measurement of water volume and water pressure unless their volumes are measured and appropriate corrections are applied. The dimensions of the pedestal and the loading cap, as well as the specimen are shown in Fig. 2.

The total volume change of the specimen can be estimated from the inflow and outflow water volumes when the speci-

[1] Manufactured by Miller-Stephenson Chemical Co., Inc., Danbury, Conn.

**Fig. 3.** Control board, plumbing layout for the permeability tests. (Direction of water movement during the permeability tests and during flushing diffused air also indicated.)

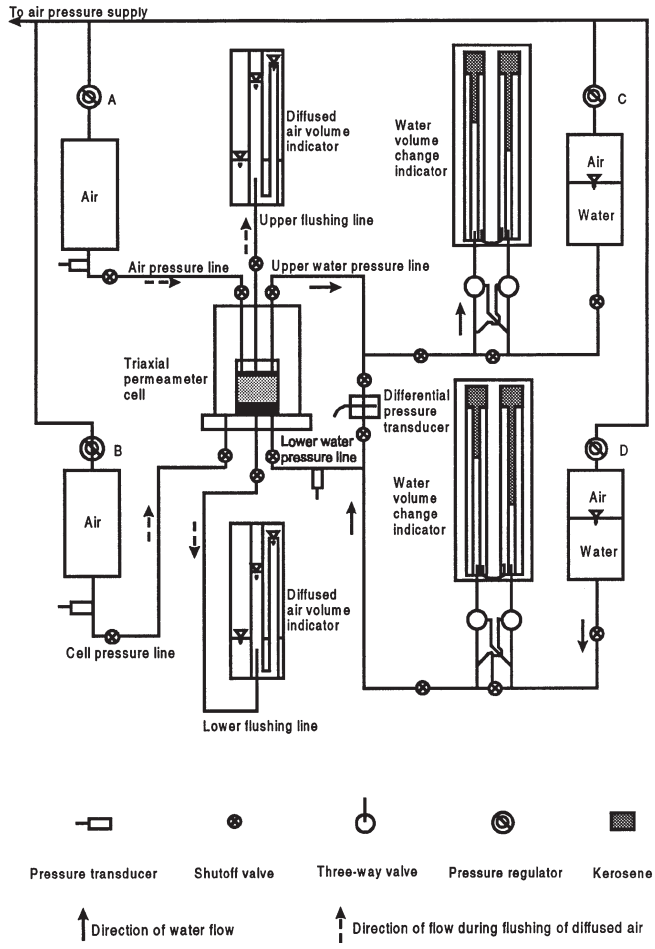


men is saturated; however, this method is no longer valid when the specimen becomes unsaturated. The total volume change of the unsaturated specimen can be measured by monitoring the deformation of the specimen using a "non-contacting displacement measuring system."[2] Two non–contacting displacement transducers were placed across the diameter of the specimen to measure changes in the diameter (Figs. 1and 2). A third noncontacting displacement transducer was installed vertically to monitor changes in the height of the specimen. For the laterally placed transducers, aluminum foil targets were attached to the rubber membrane opposite the transducers. For the vertically installed transducer, the aluminum foil target was placed on the bottom of an overturned porcelain cup, glued to the top of the loading cap. The aluminum targets were made from four folds of 20 mm squares of heavy-duty commercial aluminum foil which was $8 \times 10^{-3}$-mm thick.. The aluminum foil was compressed before use to reduce the deformation of the targets. The displacement measuring system is based on the eddy-current loss principle between a conductive surface (e.g., the aluminum targets) and the electronic transducers (Ho 1988).

## Control board and plumbing layout

The plumbing layout for the triaxial permeameter cell is shown in Fig. 3. The upper pore-water pressure line is controlled by regulator C. The air pressure is transferred to a water pressure in a half-filled water tank which, in turn, is transmitted through the upper volume change indicator, and applied to the top of the specimen through the upper high air-entry disk. The lower pore-water pressure line is controlled by regulator D in a manner similar to that used for the top cap.

The air pressure line is controlled by regulator A and monitored using a pressure transducer. The compressed air is applied to the specimen through the pore-air pressure groove on the loading cap. The cell pressure line is controlled by regulator B and monitored by a pressure transducer. The cell pressure acts as a confining pressure on the specimen.

The upper and lower flushing lines were designed such that diffused air could be flushed from the water compartments located in the loading cap and in the pedestal. Diffused air bubbles will produce errors in the measurement of the inflow and outflow water.

The pore-water pressures applied to the upper and lower ends of the specimen were set to different values to establish a hydraulic gradient across the specimen. The distribution of the pore-water pressure is not linear when the specimen is unsaturated. However, given that the applied differential pressure was limited to a range 2–4 kPa, it would appear reasonable to assume a linear pore-water pressure distribution within the specimen. The average value of the matric suction at the top and bottom of the specimen was taken as representative of the matric suction within the specimen with the hydraulic gradient across the specimen calculated from the differential pressures.

The lower pore-water pressure is monitored using a pressure transducer (Fig. 3) and the differential pressure between the top and bottom of the specimen was measured using a precision "differential pressure transducer."[3] The differential pressure transducer has a range of ±14 kPa and a resolution of 0.015 kPa. The upper pore-water pressure is obtained by combining the lower pore-water pressure and the differential pressure.

Conventional twin-burette volume change indicators were installed on the upper and lower pore-water pressure lines to independently measure inflow and outflow water volumes. The burettes in the volume change indicators have a range of 10 $cm^3$ and a resolution of 0.02 $cm^3$. The diffused air bubbles were periodically flushed from the pore-water pressure compartments into the diffused air volume indicators for measurement. The direction of the water movement during a permeability test is shown in Fig. 3.

The inflow and outflow water volumes induce changes in the elevations of the water/kerosene interfaces within the volume change indicators. These changes produce a change in the differential pressure applied to the specimen due to

[2] Manufactured by the Kaman Sciences Corporation, Colorado Springs, Col.
[3] Manufactured by Instruments Division, Bell & Howell Corporation and sold by Servo Systems Corporation, Montville, NJ, U.S.A.

**Fig. 4.** Typical differential head versus elapsed-time curves.

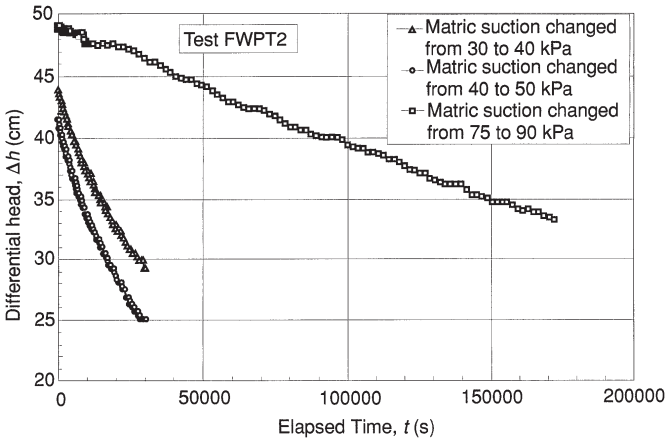


the difference between the densities of water and kerosene. Therefore, the differential pressure transducer is not only used to measure the initial differential pressure but also to monitor any change in the differential pressure. Typical curves of differential head versus elapsed time are shown in Fig. 4. The differential head decreases approximately linearly with time during the test. The mean differential head used for the coefficient of permeability calculations was determined using the mean value over a specified time interval (i.e., $\Delta h = \int_{t_1}^{t_2} \Delta h\ (t)\ dt/(t_2 - t_1)$). In general, this mean differential head is slightly lower than the arithmetic mean value of the initial and final differential heads (i.e., $\Delta h = (\Delta h_1 + \Delta h_2)/2$).

The pressure transducers, along with the strain transducers, were connected to a data acquisition system (Rahardjo 1990). Data were recorded and stored in a floppy disk using a microcomputer and the "Notebook"[4] interface program was used to sort the data. Pressure and deformation data were displayed on the monitor for observation during testing. The burette water change readings were taken manually.

### Performance of the triaxial permeameter system

All components of the triaxial permeameter system were calibrated prior to testing. The air-entry value and the coefficient of permeability for the high air-entry disks were also measured.

Effort was taken to ensure no leakage from the triaxial permeameter system. A three-month period of observations demonstrated that there was little leakage from the external plumbing connections to the triaxial permeameter cell. There was a small amount of leakage in the plumbing connections within the cell even though silicon rubber sealant was applied as a seal to the connection joints. Fortunately, the air leakage from the joints inside the cell could be flushed and measured, together with the diffused air from the high air-entry disks. The main leakage came from the gaps between the rubber membrane and the upper cap or lower pedestal. Observations made under a pressure difference of 200 kPa (i.e., 230 kPa cell pressure and 30 kPa pore-water pressure) showed that the leakage was in the range 0.14–0.25 $cm^3$/day when 50 mm diameter O-rings were used.

**Table 1.** Index properties for the soil tested (Rahardjo 1990).

| | | | |
|---|---|---|---|
| $G_s$ (%) | 2.68 | Silt (%) | 37.5 |
| $w_L$ | 22.2 | Clay (%) | 10 |
| $w_P$ | 16.6 | $D_{10}$ (mm) | 0.002 |
| PI | 5.6 | $D_{30}$ (mm) | 0.02 |
| Sand | 52.5 | $D_{60}$ (mm) | 0.09 |

Air leakage due to the difference in the cell air pressure and the pore-water pressure directly affects the accuracy of the inflow and outflow water volume measurements when the specimen is saturated. The effect of this air leakage is significantly reduced when the specimen becomes unsaturated and new air channels develop within the specimen when the matric suction exceeds the air-entry value of the specimen. The air leakage from the cell then mixes with the air within the specimen and tends to increase the pore-air pressure. However, the pore-air pressure was controlled and maintained at a constant value. As a result, the leakage of air affects neither the water flow volumes nor the matric suction when the specimen is unsaturated. For the saturated case, the influence of air leakage is small since the duration of the permeability measurements is only about 2 h (i.e., the leakage is in the order of 0.02 $cm^3$).

The observations showed that the triaxial permeameter system performed well and is reliable for measuring the coefficient of permeability for a saturated soil with a coefficient of permeability as low as $5 \times 10^{-11}$ m/s, with an error less than a ±18%. For an unsaturated soil with continuous air channels, the measurable coefficient of permeability using the triaxial permeameter would be lower than $5 \times 10^{-11}$ m/s.

Air leakage influences computations of the water content or the degree of saturation of the specimen. Air leakage does not significantly influence the accuracy of the permeability measurements since the water content or the degree of saturation is estimated from the accumulated inflow and outflow water volumes. The accumulated leakage is also included in the accumulated inflow and outflow data so that a significant error may be introduced into the computation of the water content or the degree of saturation. It appears that the coefficient of permeability function and the soil–water characteristic curve cannot be readily obtained using only a permeability test (Brooks and Corey 1964; Laliberte et al. 1966).

## Testing material

A silty sand from a Saskatchewan Department of Highway pit (South half of the legal land description of 13-18-18-W2) was selected for the test program. The index properties of the soil are shown in Table 1 (Rahardjo 1990). All specimens for the experimental program were prepared by adding distilled water to air-dried soil to produce a slurry with a gravimetric water content of approximately 24%.

[4] Produced by Laboratory Technologies Corporation, Wilmington, Mass.

**Table 2.** Stress state variables for the flexible–wall permeability tests.

| Test step | Stress state variable (kPa) | FWPT 1 (kPa) | FWPT 2 (kPa) | FWPT 3 (kPa) | FWPT 4 (kPa) | FWPT 5 (kPa) | FWPT 6 (kPa) |
|---|---|---|---|---|---|---|---|
| 0–8 | Total stress ($\sigma - u_a$) | 10 | 10 | 25 | 50 | 100 | 200 |
| 0 | Matric suction ($u_a - u_w$) | 0 | 0 | 0 | 0 | 0 | 0 |
| 1 | Matric suction ($u_a - u_w$) | 10 | 10 | 10 | 10 | 20 | 30 |
| 2 | Matric suction ($u_a - u_w$) | 20 | 20 | 20 | 20 | 30 | 40 |
| 3 | Matric suction ($u_a - u_w$) | 30 | 30 | 30 | 30 | 40 | 50 |
| 4 | Matric suction ($u_a - u_w$) | 40 | 40 | 40 | 40 | 50 | 60 |
| 5 | Matric suction ($u_a - u_w$) | 50 | 50 | 50 | 50 | 60 | 75 |
| 6 | Matric suction ($u_a - u_w$) | — | 60 | 60 | 60 | 75 | 90 |
| 7 | Matric suction ($u_a - u_w$) | — | 75 | 75 | 75 | 90 | — |
| 8 | Matric suction ($u_a - u_w$) | — | 90 | 90 | 90 | — | — |

**Table 3.** Summary of the volume–mass properties for the flexible-wall permeability tests.

| Test number | FWPT1 | FWPT2 | FWPT3 | FWPT4 | FWPT5 | FWPT6 |
|---|---|---|---|---|---|---|
| Initial void ratio, $e_i$ | — | 0.646 | 0.642 | 0.652 | 0.638 | 0.647 |
| Consolidation void ratio, $e_c$ | — | 0.536 | 0.514 | 0.507 | 0.478 | 0.468 |
| Final void ratio, $e_f$ | — | 0.522 | 0.514 | 0.502 | 0.484 | 0.467 |
| Final water content, $w_f$ (%) | — | 9.58 | 9.64 | 9.90 | 9.88 | 10.06 |
| Consolidation pressure, $\sigma_c$ (kPa) | 10 | 10 | 25 | 50 | 100 | 200 |

## Testing procedure

The axis-translation technique (Hilf 1956) was used during the permeability measurements to prevent the cavitation of water in the measuring system. The triaxial permeameter can be used to conduct a flexible-walled or a rigid-walled permeability test by using either a rubber membrane or a stainless steel sample ring, respectively (Huang 1994). The testing procedures for these two types of tests are essentially the same. Only the procedure for the flexible-walled permeability test is presented. The flexible-wall permeability tests were conducted to measure the coefficient of permeability and total volume change at different net normal stresses and matric suction levels.

The 1-bar high air-entry disks in the triaxial permeameter were saturated. A slurried specimen was then assembled into the triaxial permeameter cell using a specially designed sampler (Huang 1994). The procedure used to assemble the specimen was similar to that used in a conventional triaxial test on cohesionless soils. Filter paper was used to prevent the soil particles from filling the pore-air pressure groove on the loading cap. After the specimen was assembled, the following procedure was followed:

(1) The specimen was isotropically consolidated to the desired confining pressure. The total volume change of the specimen was measured during consolidation using both the volume change indicators and the noncontacting displacement transducers.

(2) The saturated coefficient of permeability was measured by applying a differential head to both ends of the specimen. The inflow and outflow water volumes were monitored. The differential head was also applied during consolidation to maintain an approximately constant stress state in the specimen. The readings for the inflow and outflow volumes were taken regularly from the volume change indicators. Once the difference between the inflow and outflow water volumes was small (i.e., less than 5% of the average flow volume), consolidation was considered to be complete. The saturated coefficient of permeability can be calculated using the data obtained during the corresponding time interval.

(3) The matric suction was then increased while the net normal stress was maintained constant. To produce monotonic loading, both the pore-air pressure and the confining pressure were increased gradually and simultaneously by the same amount.

(4) The specimen was allowed to desaturate under the applied matric suction. A differential head was also simultaneously applied to both ends of the specimen. The total volume change and the inflow and outflow water volumes were monitored. Once the difference between the inflow and outflow water volumes for a particular time interval was small (i.e., less than 5% of the average flow volume), the specimen was considered to be at equilibrium under the applied matric suction. The data obtained from this particular period were used to calculate the coefficient of permeability at the applied matric suction based on Darcy's Law and steady-state flow. The volume of diffused air had to be regularly flushed (i.e., approximately every 12 h) and measured. Appropriate corrections were applied to the inflow and outflow water volumes.

(5) Steps (3) and (4) were repeated at higher matric suction values for the same specimen until the matric suction reached 90 kPa, which was 10 kPa lower than the air-entry value of the high air-entry disks as specified by the manufacturer.

The above procedure was repeated for each of the six specimens. Each specimen was subjected to a different con-

**Fig. 5.** Void ratio change versus matric suction obtained from flexible-wall permeability tests.

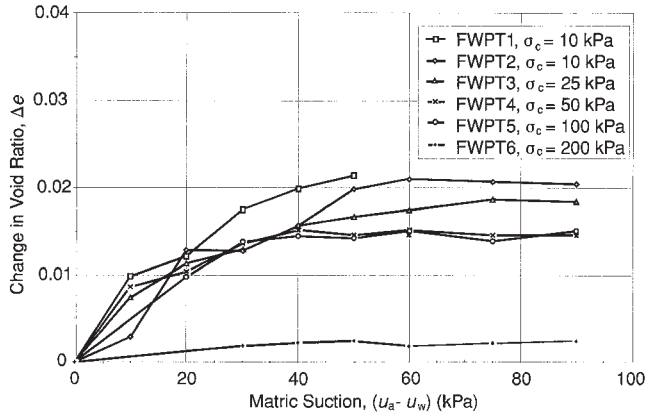


**Fig. 6.** Coefficient of permeability versus matric suction obtained from flexible-wall permeability tests.

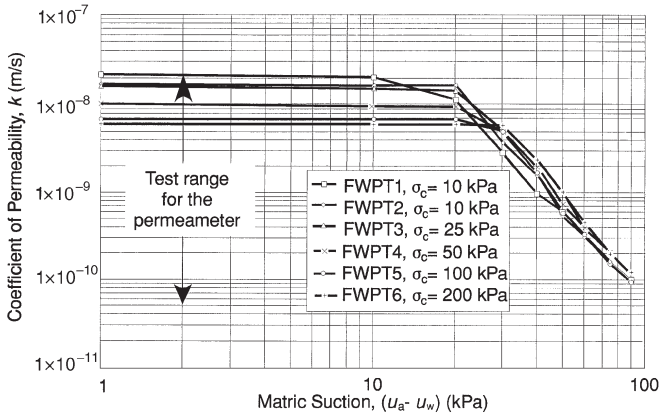


fining pressure. Approximately 4 weeks were required to test each specimen.

## Test results

Six flexible-wall permeability tests (i.e., FWPT1 to FWPT6) were conducted using the developed triaxial permeameter. The stress states used in each test are presented in Table 2. The volume–mass properties are summarized in Table 3.

The first test, FWPT1, was conducted as a pilot test. The equipment performed well until the matric suction reached 50 kPa. The high air-entry disk on the pedestal had been accidentally damaged during testing. Consequently, the air-entry value of the disk was greatly reduced. When the matric suction approached 50 kPa, air penetrated the cracks in the high air-entry disk and a considerable volume of air was collected in the diffused air volume indicator. The test was stopped at this matric suction. An attempt was made to remove the specimen after the test. Unfortunately, it was still in a slurried state and the volume–mass properties were difficult to obtain. The remaining five tests were conducted after a new high air-entry disk was sealed onto the base plate. The equipment performed well for the remainder of the tests.

The measurements of the total volume of the specimens indicated that the total volume change could not be monitored with sufficient accuracy. This became apparent when the total volume changes obtained during consolidation were compared to the outflow water volume during the same time period. The total volume changes measured using the noncontacting displacement transducers over-estimated the actual total volume change (i.e., up to 50% higher than the values obtained from outflow water volume). Nonuniform deformations of the specimens are likely responsible for the low accuracy in the measurements. The middle section of the specimen deformed the most while the ends deformed less, due likely to friction between the loading cap and the pedestal. The situation was worse at high confining pressures. The rate of total volume change seems to be reasonable but the total volume changes appear to be high.

The void-ratio changes referenced to the zero matric suction state (i.e., after consolidation) for all six specimens are shown in Fig. 5. The results show that the change in void ratio is complete when the matric suction reaches approximately 30 kPa. Soil–water characteristic curves measured on this material produced an air-entry value of approximately 30 kPa (Huang et al. 1998). As the matric suction increases further, the void ratio does not change significantly. It can likewise be concluded that the void ratio or total volume change in the consolidated slurried silt specimen was not significant, particularly under high consolidation pressures.

The coefficients of permeability versus matric suction relationships are presented in Fig. 6. The coefficient of permeability does not change significantly when the matric suction is low. As the matric suction increases beyond the air-entry value of the soil the coefficient of permeability decreases rapidly. The coefficients of permeability versus matric suction data follow a bi-linear relationship on a log-log scale, similar to Brooks and Corey (1964).

## Conclusions

The developed triaxial permeameter system is suitable for measuring the coefficient of permeability of a saturated soil with a coefficient of permeability as low as $5 \times 10^{-11}$ m/s. At the lowest possible coefficient of permeability, the error would be in the order of ±18%. For an unsaturated soil the measurable coefficient of permeability can be much lower than $5 \times 10^{-11}$ m/s. The highest coefficients of permeability that can be measured are those approximating the coefficient of permeability of the ceramic disks (i.e., $2 \times 10^{-8}$ m/s). The total volume change measurements using strain transducers were not sufficiently accurate due possibly to nonuniform deformation throughout the soil specimen. The deformation transducers do, however, provide a qualitative indication of the relative rate and magnitude of volume changes due to changes in matric suction.

The coefficient of permeability of the soil does not decrease significantly as the matric suction increases from zero to the air-entry value, although the total volume of the sample underwent some change. When the matric suction value exceeds the air-entry value, the coefficient of permeability decreases sharply while the total volume does not change significantly. The coefficient of permeability versus matric suction relationship appears to be bilinear on a log–log

scale. The total volume change due to the matric suction change is generally small for the consolidated slurried specimens of silty sand.

## References

Barden, L., and Pavlakis, G. 1971. Air and water permeability of compacted unsaturated cohesive soil. Journal of Soil Science, **22**: 302–317.

Brooks, R.H., and Corey, A.T. 1964. Hydraulic properties of porous media. Hydrology Paper, No. 3, Colorado State University, Fort Collins, Col.

Corey, A.T. 1957. Measurement of water and air permeability in unsaturated soil. Proceedings, Soil Science Society of America, **21**: 7–10.

Fredlund, D.G., and Rahardjo, H. 1993. Soil mechanics for unsaturated soils. John Wiley & Sons, Inc., New York.

Hilf, J.W. 1956. An investigation of pore-water pressure in compacted cohesive soils. Ph.D. thesis, Technical Memo No. 654, U.S. Department of the Interior, Bureau of Reclamation, Design and Construction Division, Denver.

Ho, D.Y.F. 1988. The relationship between the volumetric deformation moduli of unsaturated soils. Ph.D. thesis, Department of Civil Engineering, University of Saskatchewan, Saskatoon, Sask.

Huang, S.Y. 1994. Evaluation and laboratory measurement of the coefficient of permeability in deformable, unsaturated soils. Ph.D. thesis, University of Saskatchewan, Saskatoon, Sask.

Huang, S.Y., Barbour, S.L., and Fredlund, D.G. 1998. Development and verification of a coefficient of permeability function for a deformable, unsaturated soil. Canadian Geotechnical Journal **35:** 411–425.

Klute, A. 1965. Laboratory measurement of hydraulic conductivity of unsaturated soils. *In* Methods of soil analysis. *Edited by* C.A. Black, D.D. Evans, J.L. White, L.E. Ensminger, and F.E. Clark. Monograph 9, Part 1, American Society of Agronomy, Madison, Wis. pp. 253–261.

Klute, A. 1972. The determination of the hydraulic conductivity and diffusivity of unsaturated soils. Soil Science, **113**: 264–276.

Klute, A., and Dirksen, H.E. 1986. Hydraulic conductivity and diffusivity: laboratory methods. *In* Method of Soil Analysis. *Edited by* A. Klute. Part 1. American Society of Agronomy, Madison, Wis. pp. 687–734.

Laliberte, G.E., Corey, A.T., and Brooks, R.H. 1966. Properties of unsaturated porous media. Hydrology paper No. 17, Colorado State University, Fort Collins, Col.

Rahardjo, H. 1990. The study of undrained and drained behavior of unsaturated soils. Ph.D. thesis, University of Saskatchewan, Saskatoon, Sask.